Methyl dynamics of a Ca2+−calmodulin−peptide complex from NMR/SRLS

ARTICLE *in* THE JOURNAL OF PHYSICAL CHEMISTRY B · JANUARY 2011

Impact Factor: 3.3 · DOI: 10.1021/jp107130m · Source: PubMed

4 AUTHORS, INCLUDING:

Yury E. Shapiro
Bar Ilan University
180 PUBLICATIONS **865** CITATIONS
SEE PROFILE

Antonino Polimeno
University of Padova
124 PUBLICATIONS **1,551** CITATIONS
SEE PROFILE

Methyl Dynamics of a Ca^{2+}−Calmodulin−Peptide Complex from NMR/SRLS

Yury E. Shapiro,*,† Antonino Polimeno,‡ Jack H. Freed,§ and Eva Meirovitch*,†

The Mina and Everard Goodman Faculty of Life Sciences, Bar-Ilan University, Ramat-Gan 52900, Israel, Department of Physical Chemistry, University of Padua, 35131 Padua, Italy, and Baker Laboratory of Chemistry and Chemical Biology, Cornell University, Ithaca, New York 14853-1301, United States

Received: July 29, 2010; Revised Manuscript Received: November 21, 2010

We developed the slowly relaxing local structure (SRLS) approach for analyzing NMR spin relaxation in proteins. SRLS accounts for dynamical coupling between the tumbling of the protein and the local motion of the probe and for general tensorial properties. It is the generalization of the traditional model-free (MF) method, which does not account for mode-coupling and treats only simple tensorial properties. SRLS is applied herein to ^{2}H relaxation of $^{13}CDH_2$ groups in the complex of Ca^{2+}−calmodulin with the peptide smMLCKp. Literature data comprising ^{2}H T_1 and T_2 acquired at 14.1 and 17.6 T, and 288, 295, 308, and 320 K, are used. We find that mode-coupling is a small effect for methyl dynamics. On the other hand, general tensorial properties are important. In particular, it is important to allow for the asymmetry of the local spatial restrictions, which can be represented in SRLS by a rhombic local ordering tensor with components S_0^2 and S_2^2. The principal axes frame of this tensor is obviously different from the axial frames of the magnetic tensors. Here, we find that $-0.2 \leq S_0^2 \leq 0.5$ and $-0.4 \leq S_2^2 \leq 0$. MF features a single "generalized" order parameter, S, confined to the 0−0.316 range; the local geometry is inherently simple. The parameter S is inaccurate, having absorbed unaccounted for effects, notably $S_2^2 \neq 0$. We find that the methionine methyls (the other methyl types) reorient with rates of 8.6×10^9 to 21.4×10^9 (0.67×10^9 to 6.5×10^9) 1/s. The corresponding activation energies are 10 (10−27) kJ/mol. By contrast, MF yields inaccurate effective local motional correlation times, τ_e, with nonphysical temperature dependence. Thus, the problematic S- and τ_e-based MF picture of methyl dynamics has been replaced with an insightful physical picture based on a local ordering tensor related to structural features, and a local diffusion tensor that yields accurate activation energies.

1. Introduction

NMR spin relaxation is a powerful method for elucidating protein dynamics.[1−13] ^{15}N spin relaxation of the N−H bond is typically used to study backbone dynamics,[1−5,7−10] and ^{2}H spin relaxation of the $^{13}CDH_2$ methyl group[5,6,11−13] to study side-chain dynamics. We developed in recent years the slowly relaxing local structure (SRLS) approach[14−16] for analyzing NMR spin relaxation in proteins.[17−19] So far, SRLS has been implemented in the overdamped diffusion limit within the scope of a two-body coupled-rotator formalism. SRLS accounts for dynamical coupling between the local motion of the NMR probe and the global motion of the protein, and allows for general properties of the second rank tensors involved. Here, we focus on methyl dynamics in the complex of Ca^{2+}−calmodulin with the peptide smMLCKp (GSARRKWQKTGHAVRAIGRLS), denoted Ca^{2+}-CaM*smMLCKp. Literature data comprising ^{2}H T_1 and T_2 acquired at 14.1 and 17.6 T, and 288, 295, 308, and 320 K,[20] are analyzed with SRLS.

Methyl dynamics probed with $^{13}CDH_2$ (cf. ref 11) is inherently more challenging than backbone dynamics probed with ^{15}N−^{1}H.[21] Both have been treated mostly with the model-free (MF) approach.[22−24] While the local restrictions at the N−H bond may be modeled as axial confinement around the equilibrium N−H orientation,[22] this picture is not applicable to methyl motion. It was shown in early work that axial confinement around the C−CH_3 bond, accounted for straightforwardly within the scope of Woessner's model,[25] does not explain experimental data from proteins.[26] Rather, nonaxial restrictions on the motion of this bond must also be accounted for.[26] Thus, although the local motion of the methyl group is typically much faster than the global tumbling (hence largely decoupled from it),[6,27−30] as assumed in MF, appropriate treatment of methyl dynamics requires accounting for general tensorial properties. MF cannot account for these properties.

Unlike the ^{15}N nucleus in the ^{15}N−^{1}H probe, the ^{2}H nucleus in the $^{13}CDH_2$ probe is not bound chemically to ^{1}H. Hence, the important high-frequency values of the spectral density, supplied by heteronuclear NOEs, are not available. Only the spectral density values of $J^{QQ}(0)$, $J^{QQ}(\omega_D)$, and $J^{QQ}(2\omega_D)$ (Q denotes the quadrupole tensor and ω_D the ^{2}H Larmor frequency) enter the expressions for the experimental relaxation parameters, typically ^{2}H T_1 and T_2.[11] Finally, the T_2 values of the quadrupole ^{2}H nucleus are small, and often quite similar at different magnetic fields.

In SRLS, the local restrictions are represented by a (coupling/ordering) potential of mean force (POMT). The simplest representation of the actual nonaxial local ordering scenario is through a rhombic POMT with the main local ordering axis lying along the C−CDH_2 bond, i.e., tilted at 110.5° from the (axial) quadrupolar frame (this value of the tetrahedral carbon angle corresponds to $r_{CH} = r_{CD} = 1.115$ Å, used in methyl HH−HC cross-correlation studies[27]).

This model was suggested by us previously and applied to experimental data.[28,29] For simplicity, we considered the local diffusion tensor, $\boldsymbol{R}^L$, to be isotropic. In the present study, we

* Corresponding authors. E-mail: shapiro@nmrsgi4.ls.biu.ac.il (Y.E.S.), eva@nmrsgi5.ls.biu.ac.il (E.M.).
† Bar-Ilan University.
‡ University of Padua.
§ Cornell University.

10.1021/jp107130m
Published on Web 12/17/2010

investigate the temperature dependence of the local motional rates, R^L, and of the axial and rhombic coefficients of the POMT, c_0^2 and c_2^2. Activation energies are derived from R^L.

Methyl dynamics has been analyzed traditionally with the model-free (MF) approach.[6,11−13] The formal MF analogue of $\tau = 1/(6R^L)$ is the effective local motional correlation time, τ_e. This parameter is typically inaccurate; in some cases, it is not even reported.[20] Often τ_e does not exhibit any temperature dependence. Therefore, activation energies for local motion have only been reported for a small number of methyl groups studied over narrow temperature ranges.[30] We show herein that R^L derived with SRLS exhibits Arrhenius-type temperature dependence over a substantial temperature range, enabling the determination of activation energies for virtually all the experimentally studied methyl groups of Ca^{2+}-CaM*smMLCKp. Information specific to the type of the methyl group is obtained. For example, we find that methionine methyl groups reorient on average six times faster, and have on average two times lower activation energies for local motion, than all the other methyl groups. The ultimate objective is to correlate the activation energies with the local structure.

Another physical quantity examined in detail in the present study is the POMT. Its form represents useful structural information. The first step, pursued herein, is to characterize the POMT and the associated local ordering tensor. The next step, to be pursued in future studies, is to correlate this information with the structure of the protein. Here, we show that the local motional rates and their activation energies, as well as the form and characteristics of the POMT, provide a clear and insightful mesoscopic picture of structural methyl dynamics in proteins.

The SRLS time correlation functions (TCFs) are obtained by solving numerically the two-body Smoluchowski equation.[17−19] The measurable spectral densities are obtained by linearly combining the generic spectral densities (which are Fourier transforms of the TCFs) in accordance with the local geometry. The SRLS TCFs comprise a sum of multiple weighted exponents that correspond to the eigenmodes of motion. The weighting factors, which represent the contribution of each eigenmode, depend upon the local and global diffusion tensors, and the POMT. We illustrate herein typical SRLS TCFs for methyl dynamics and compare with the MF TCF. Note that TCFs for restricted motions in locally ordered media are also given by sums of multiple weighted exponents;[31] the respective theories, and SRLS, are based on the same principles (cf. ref 19).

Finally, we examine the nature of the MF spectral density used to treat methyl dynamics, and the significance of the parameters that enter it. The main qualifier is S_{axis}^2, interpreted as the amplitude of the $C-CH_3$ fluctuations. This parameter is given by the ratio of a squared "generalized" order parameter, S^2, and a trigonometric coefficient, 0.1,[25] associated with a frame transformation.[19] In contrast, in the classical theories for treating restricted motions in liquids (e.g., refs 14−16 and 31), order parameters (or more precisely tensors) are defined in terms of orienting potentials. They assess the preferential orientation of the local ordering frame in the (local) director frame; this represents important structural information. The quantities S and S_{axis} are artificial parameters both by definition[22] and in practice because they absorb unaccounted for effects.[28,29] Therefore, their physical meaning is vague.

Three groups of S_{axis}^2 values, centered at 0.2, 0.4, and 0.8, have been observed in MF analyses.[32] This classification has been interpreted as a manifestation of the microscopic nature of entropy in proteins.[32] We show that these groups of S_{axis}^2 values are just associated with different forms of the POMT, which the SRLS analysis effectively correlates with different methyl types.

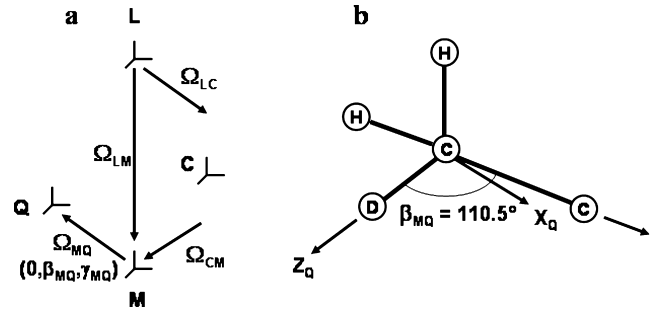

Figure 1. (a) Various reference frames that define the SRLS model. L is the laboratory frame; C is the global diffusion frame, taken isotropic in this study; M is the local ordering/local diffusion frame fixed in the C−D bond; Q is the magnetic quadrupolar dipolar frame fixed in the C−D bond; Ω_{LC} are Ω_{CM} are time-dependent Euler angles associated with the global motion and the relative local motion, respectively. (b) Methyl group schematic corresponding to a rhombic local ordering scenario with $\beta_{MQ} = 110.5°$ and $\gamma_{MQ} = 0°$. Within a good approximation, this represents "X-ordering". The main ordering axis lies along the $C-CDH_2$ bond.

We give a short Theoretical Background section followed by Results and Discussion, and then Conclusions.

2. Theoretical Background

2.1. Slowly Relaxing Local Structure (SRLS) Approach. The fundamentals of the stochastic coupled rotator slowly relaxing local structure theory, as applied to NMR spin relaxation in proteins, have been presented and reviewed previously.[17−19] The application to methyl dynamics is described in refs 28 and 29. A brief summary is given below for convenience.

The SRLS frames for methyl dynamics are shown in Figure 1a. L is the space-fixed laboratory frame with its Z-axis aligned along the external magnetic field, B_0. C is the global diffusion frame fixed in the protein. In this study, we consider the latter to be isotropic; hence, C also serves as local director. Q is the (axial) magnetic quadrupolar frame fixed in the probe. M is the (rhombic) local ordering/local diffusion frame fixed in the probe. The orientation of the M frame is not known a priori. In general, it is determined by data fitting. Figure 1b illustrates the scenario wherein $\beta_{MD} = 110.5°$ and $\gamma_{MD} = 0°$. Within a good approximation, this represents "X-ordering", with the main ordering axis lying along the $C-CDH_2$ bond.

The time-dependent Euler angles, $\Omega_{LM}(t)$, are modulated by the local and global motions. The time-dependent Euler angles, $\Omega_{LC}(t)$, are modulated by the global tumbling. For describing the local motion we use a relative (probe versus protein) coordinate scheme; that is, $\Omega_{CM}(t) = \Omega_{LM}(t) - \Omega_{LC}(t)$.[18,19] The two rotators are coupled by the POMT, $U(\Omega_{CM})$. The diffusion equation for the coupled system is given by

$$\frac{\partial}{\partial t}P(X,t) = -\hat{\Gamma}P(X,t) \qquad (1)$$

where X is a set of coordinates completely describing the system. One has[18,19]

$$X = (\Omega_{CM}, \Omega_{LC})$$
$$\Gamma = \hat{J}(\Omega_{CM})\mathbf{R}^{L}P_{eq}\hat{J}(\Omega_{CM})P_{eq}^{-1} + [\hat{J}(\Omega_{CM}) - \hat{J}(\Omega_{LC})]\mathbf{R}^{C}P_{eq}[\hat{J}(\Omega_{CM}) - \hat{J}(\Omega_{LC})]P_{eq}^{-1} \quad (2)$$

where $\hat{J}(\Omega_{CM})$ and $\hat{J}(\Omega_{LC})$ are the infinitesimal rotation operators for the probe and the protein, respectively.

The Boltzmann distribution is $P_{eq} = \exp[-U(\Omega_{CM})/k_BT]/\langle\exp[-U(\Omega_{CM})/k_BT]\rangle$. The potential $U(\Omega_{CM})$ is in general expanded in the full basis set of the Wigner rotation matrix elements. In this study only the $L = 2$ terms are preserved:[18,19,28,29]

$$u(\Omega_{CM}) = \frac{U(\Omega_{CM})}{k_BT} \approx -c_0^2D_{0,0}^2(\Omega_{CM}) - c_2^2[D_{0,2}^2(\Omega_{CM}) + D_{0,-2}^2(\Omega_{CM})] \quad (3)$$

The coefficient c_0^2 is related to the strength of the POMT, and c_2^2 is related to its nonaxiality. The order parameters, $S_0^2 = \langle D_{00}^2(\Omega_{CM})\rangle$ and $S_2^2 = \langle D_{02}^2(\Omega_{CM}) + D_{0-2}^2(\Omega_{CM})\rangle$, are calculated from c_0^2 and c_2^2 according to[18,19]

$$\langle D_{0n}^2(\Omega_{CM})\rangle = \int d\Omega_{CM}\, D_{0n}^2(\Omega_{CM}) \times \exp[-u(\Omega_{CM})]/\int d\Omega_{CM}\exp[-u(\Omega_{CM})] \quad (4)$$

The Cartesian ordering tensor components are given by $S_{zz} = S_0^2$, $S_{xx} = (\sqrt{(3/2)}S_2^2 - S_0^2)/2$, $S_{yy} = -(\sqrt{(3/2)}S_2^2 + S_0^2)/2$, with $S_{xx} + S_{yy} + S_{zz} = 0$.

Expansion terms corresponding to $L = 4$, $K = 0$, 2, 4, (c_0^4, c_2^4, and c_4^4) are included in our most recent computational scheme.[33] They allow a more detailed modeling, in particular diffusion within two wells with less frequent jumps between them.[15,34] More general jump models and modeling may be included by adding appropriate terms in the expansion of $U(\Omega_{CM})$. This is relevant for more complex methyl dynamics, to be considered in future work.

Equation 2 is solved to yield the SRLS time correlation functions which lead by Fourier transformation to the spectral densities, $j_{K,K'}(\omega) = \sum_i(c_{K,K',i}\tau_i)/(1 + \omega^2\tau_i^2)$.[18,19] The relevant pairs, K,K', are determined by the symmetry of the local ordering/local diffusion and magnetic tensors. In practice, a finite number of terms is sufficient for numerical convergence of the solution.

The $j_{K,K'}(\omega)$ functions are assembled into the measurable spectral density, $J^{QQ}(\omega)$, according to the local geometry.[17−19] For ^{2}H relaxation in the presence of a rhombic POMT only six pairs, $K,K' = 0,0$; 1,1; 2,2; 2,0; 1,−1; and 2,−2, persist. One has[28,29]

$$J^{QQ}(\omega) = (d_{00}^2(\beta_{MQ}))^2j_{00}(\omega) + 2(d_{10}^2(\beta_{MQ}))^2j_{11}(\omega) + 2(d_{20}^2(\beta_{MQ}))^2j_{22}(\omega) + 4d_{00}^2(\beta_{MQ})d_{20}^2(\beta_{MQ})j_{02}(\omega) + 2d_{-10}^2(\beta_{MQ})2d_{10}^2(\beta_{MQ})j_{-11}(\omega) + 2d_{-20}^2(\beta_{MQ})d_{20}^2(\beta_{MQ})j_{-22}(\omega) \quad (5)$$

Together with the magnitude of the quadrupolar interaction, the spectral density values $J^{QQ}(0)$, $J^{QQ}(\omega_D)$, and $J^{QQ}(2\omega_D)$ determine the experimentally measured relaxation rates ^{2}H T_1 and T_2, according to standard expressions for NMR spin relaxation.[11] The fitting scheme for SRLS used in this study is described in ref 18.

2.2. Model-Free. The MF approach provides directly the measurable spectral density, $J(\omega)$. The latter comprises two Lorentzian terms which represent the global motion and a single (effective) local motion.[22,23] This simple form is based on the premise that the motions considered are independent statistically because they are time scale separated. $J(\omega)$ is given in MF by:[22]

$$J(\omega) = S^2\tau_m/(1 + \tau_m^2\omega^2) + (1 - S^2)\tau'_e/(1 + \tau'^2_e\omega^2) \quad (6)$$

where τ_m is the correlation time for the global motion, $\tau_e \ll \tau_m$ is the effective correlation time for the local motion, and S^2 is the square of a "generalized" order parameter. By virtue of $\tau_e \ll \tau_m$, one has $1/\tau'_e = 1/\tau_m + 1/\tau_e \sim 1/\tau_e$. S^2 is defined as the plateau value, $C^L(\infty)$, to which the local motional time correlation function, $C^L(t)$, is assumed to converge at long times. Mathematically $C^L(\infty)$ is given by $\sum_{m=0,\pm1,\pm2}\langle|Y_{2m}(\theta,\phi)|\rangle^2$, where Y_{2m} are the spherical harmonics of Brink and Satchler.[35] $S \equiv [C^L(\infty)]^{1/2}$ is the "generalized" order parameter.

S^2 is considered to represent the amplitude of the local motion. In the context of the physical definition of order parameters (cf. eq 4), this is appropriate in the limit of a strong axial POMT, with the local motion in the extreme motional narrowing limit.[16] Based on the theory of moments, τ_e is defined as the area of the exact time correlation function for internal motion divided by $(1 - S^2)$.

The extended MF (EMF) spectral density[24] features a fast local motion, with effective correlation time, τ_f, and squared order parameters, S_f^2, and a slow local motion, with effective correlation time, τ_s, and squared order parameter, S_s^2. The three dynamic modes, represented by τ_m, τ_f, and τ_s, are assumed to be decoupled from one another. In practice, τ_s and τ_m are allowed to occur on the same time scale.[36]

In its application to methyl dynamics, eq 6 has been reinterpreted to represent two local motions. This was accomplished by factoring S into $S = [P_2(\cos 110.5°)] \times S_{axis} = 0.316S_{axis}$.[11,22,37] The factor 0.316 is considered to be the order parameter for methyl rotation around the C−CH$_3$ bond, referencing the article of Woessner.[25] S_{axis} represents the order parameter for axial fluctuations of the C−CH$_3$ bond. The correlation time, τ_e, is assigned to both local motions. The spectral density given by eq 6 is recast as

$$J^{QQ}(\omega) = 0.1 \times S_{axis}^2\tau_m/(1 + \omega^2\tau_m^2) + (1 - 0.1 \times S_{axis}^2)\tau'_e/(1 + \omega^2\tau'^2_e) \quad (7)$$

where $1/\tau'_e = 1/\tau_e + 1/\tau_m \sim 1/\tau_e$.

In the limit where $S_{axis}^2 = 1$, eq 7 should yield Woessner's model;[25] let us examine this limit. Woessner's model treats diffusive (or jump-type) motion about an axis tilted at a fixed angle, β, from an axial magnetic frame. The (tilted) diffusion axis tumbles isotropically with correlation time τ_c, the internal motion around it occurs with correlation time τ, and $\tau_c \gg \tau$. For diffusive internal motion one has two local motional decay constants, $(\tau'_1)^{-1} = \tau_c^{-1} + \tau^{-1}$ and $(\tau'_2)^{-1} = \tau_c^{-1} + 4\tau^{-1}$; for symmetrical jumps one has $(\tau')^{-1} = \tau_c^{-1} + \tau^{-1}$. For $\beta = 110.5°$, the measurable spectral density for diffusive motion is given by[25]

$$J^{QQ}(\omega) = 0.1\tau_c/(1 + \omega^2\tau_c^2) + 0.323\tau'_1/(1 + \omega^2(\tau'_1)^2) + 0.577\tau'_2/(1 + \omega^2(\tau'_2)^2) \quad (8)$$

$(d^2_{00}(110.5°))^2 = 0.1$, $2(d^2_{01}(110.5°))^2 = 0.323$, and $2(d^2_{02}(110.5°))^2 = 0.577$ are the elements of the (reduced) matrix representation of the Wigner rotation from the (axial) diffusion frame to the (axial) quadrupolar frame. The isotropic tumbling limit, $J^{QQ}(\omega) = \tau_c/(1 + \omega^2\tau_c^2)$, is obtained for $\tau \rightarrow \infty$, $\beta_{MQ} \rightarrow 0$, or both.[25]

In analogy with eq 8, eq 7 has to fulfill the relation $\tau_m \gg \tau_e$; it should not be used when τ_e and τ_m are comparable in magnitude. This is implicit in MF, but is often not appreciated.[36] Equation 7 does not converge to the isotropic tumbling limit of Woessner's model; rather, it yields $J^{QQ}(\omega) = 0.1\tau_c/(1 + \omega^2\tau_c^2)$ for $S_{axis}^2 = 1$ and $\tau_e \rightarrow 0$. The parameter τ_e represents simultaneously the internal motion in Woessner's model (τ), and restricted axial fluctuations of the C−CH_3 axis. The motion of this axis represents in Woessner's model the motion of the protein (τ_c); so does τ_m in eq 7. Clearly, τ_e is a physically vague parameter. The coefficient 0.1 in eq 7 is the trigonometric expression $(d^2_{00}(110.5))^2$. It is not an order parameter; Woessner's model does not feature an order parameter.[25] Clearly, $S_{axis}^2 = S^2/0.1$, where S is the "generalized" order parameter and 0.1 a geometric coefficient, is a physically vague quantity.

Equation 7 may not be considered to represent two restricted local motions. It represents a single diffusive local motion occurring in the presence of a weak axial POMT, with the main local ordering/local diffusion axis tilted at 110.5° from the quadrupolar frame. For this scenario one has (e.g., cf. ref 19):

$$j_{00}(\omega) = (S_0^2)^2\tau_m/(1 + \omega^2\tau_m^2) + (1 - (S_0^2))^2\tau_0/(1 + \omega^2\tau_0^2) \quad (9a)$$

$$j_{11}(\omega) = \tau_1/(1 + \omega^2\tau_1^2) \quad (9b)$$

and

$$j_{22}(\omega) = \tau_2/(1 + \omega^2\tau_2^2) \quad (9c)$$

The measurable spectral density is given by

$$\begin{aligned} J^{QQ}(\omega) &= (d^2_{00}(110.5°))^2 j_{00}(\omega) + 2(d^2_{01}(110.5°))^2 j_{11}(\omega) + \\ &\quad 2(d^2_{02}(110.5°))^2 j_{22}(\omega) \\ &= 0.1 j_{00}(\omega) + 0.323 j_{11}(\omega) + 0.577 j_{22}(\omega) \end{aligned} \quad (10)$$

Assuming that $\tau_0 = \tau_1 = \tau_2 = \tau$ (by virtue of $\tau_m \gg \tau_K$), one obtains

$$\begin{aligned} J^{QQ}(\omega) = 0.1 \times (S_0^2)^2\tau_m/(1 + \omega^2\tau_m^2) + \\ (1 - 0.1 \times (S_0^2)^2)\tau/(1 + \omega^2\tau^2) \end{aligned} \quad (11)$$

This is formally the same as eq 7 wherein S_{axis}^2 is replaced by $(S_0^2)^2$ and τ_e is replaced by τ. However, eq 11 is not suitable for describing methyl dynamics from a physical point of view because a weak axial POMT implies a broad axial distribution of the instantaneous orientation of the C−CH_3 bond about the equilibrium orientation of the C−CH_3 bond. This is difficult to rationalize for tightly packed protein cores. On the other hand, a weak but rhombic POMT, inherent in the SRLS description, is associated with a nonaxial distribution which can be accommodated, and is consistent with experimental observations.[26]

3. Results and Discussion

^2H T_1 and T_2 data of the $^{13}CDH_2$ methyl groups of Ca^{2+}-CaM*smMLCKp, acquired at 14.1 and 17.6 T, and 288, 295, 308, and 316 K,[20] were analyzed with SRLS. For a rhombic POMT and an isotropic local diffusion tensor, $\boldsymbol{R}^L$,[28,29] the variables in the data-fitting process are c_0^2, c_2^2, and $R^C = \tau/\tau_m$. Unique results are obtained by requiring that the local motional rates, $1/(6\tau)$, obey the Arrhenius relation. The global motional correlation time, τ_m, was taken from ref 20. For simplicity, the angle γ_{MQ} was set equal to zero. The angle β_{MQ} was allowed to deviate from 110.5° by 1−2°; these deviations account to some extent for the complexity of the local structure wherein the methyl group reorients. The errors in the various best-fit parameters are estimated to be on the order of 10%. The statistical measure used in our calculations is the percentile value for χ^2 distribution. The reduced χ^2, defined as χ^2/df, where df denotes the number of degrees of freedom, was in most cases below the critical 0.1 and 0.05 values.[38]

3.1. Local Motional Diffusion Rates, Activation Energies, and the POMT. Figure 2 shows the local motional correlation time, τ, and the axial (c_0^2) and rhombic (c_2^2) coefficients of the POMT, as a function of temperature for the various methyl types. For methionines, τ ranges between 7.8 and 19.5 ps; for the other methyl groups it ranges between 25.7 and 249.3 ps. On average, the methionine methyls reorient 10 times faster than the other methyl groups. In the latter category, the isoleucine δ methyls have the smallest τ values. The uniformity of τ among the various methyl types increases with increasing temperature.

Figure 3a shows the temperature dependence of the local motional rates, $R^L = 1/(6\tau)$. Virtually all the methyl groups reorient with rates that increase with increasing temperature. Figure 3b shows the activation energies, E_a, derived from the temperature dependence of R^L using the Arrhenius equation. The E_a values lie in the range of 10−27 kJ/mol. With the exception of methyl M76, which resides in the flexible interdomain linker of Ca^{2+}-CaM*smMLCKp,[39] the activation energies for the methionine methyls are approximately 10 kJ/mol.

The average value of E_a is comparable in magnitude to the average barrier height obtained for alanine methyls using molecular dynamics (MD) simulations.[40] These barrier heights are difficult to determine accurately and unambiguously.[40] The temperature dependence of τ_e MF is in most cases not amenable to analysis in terms of activation energies. Reference 20 does not report the τ_e values; we calculated them using a version of Moldelfree 4.0 (ref 41) adapted to methyl dynamics. The results obtained for the methionine methyls (which are perhaps the best candidates for normal temperature dependence) are shown in Figure 4. The corresponding τ values obtained with SRLS are shown in Figure 5. Clearly, physically meaningful information cannot be derived from the data shown in Figure 4. On the other hand, data such as those shown in Figure 5 led to accurate activation energies for virtually all the methyl groups of Ca^{2+}-CaM*smMLCKp (cf. Figure 3). Reference 30 is among the few MF studies that reported activation energies for methyl group motion in proteins. This was accomplished for selected methyl groups examined over a temperature range of 17°.[30] Although on average there was agreement with MD,[40] site-specific agreement was not obtained.

The strength of the POMT is given by the coefficient c_0^2, shown in Figure 2b; its deviation from axial symmetry is given by the coefficient c_2^2, shown in Figure 2c. The c_0^2 values are predominantly positive, whereas all the c_2^2 values are negative.

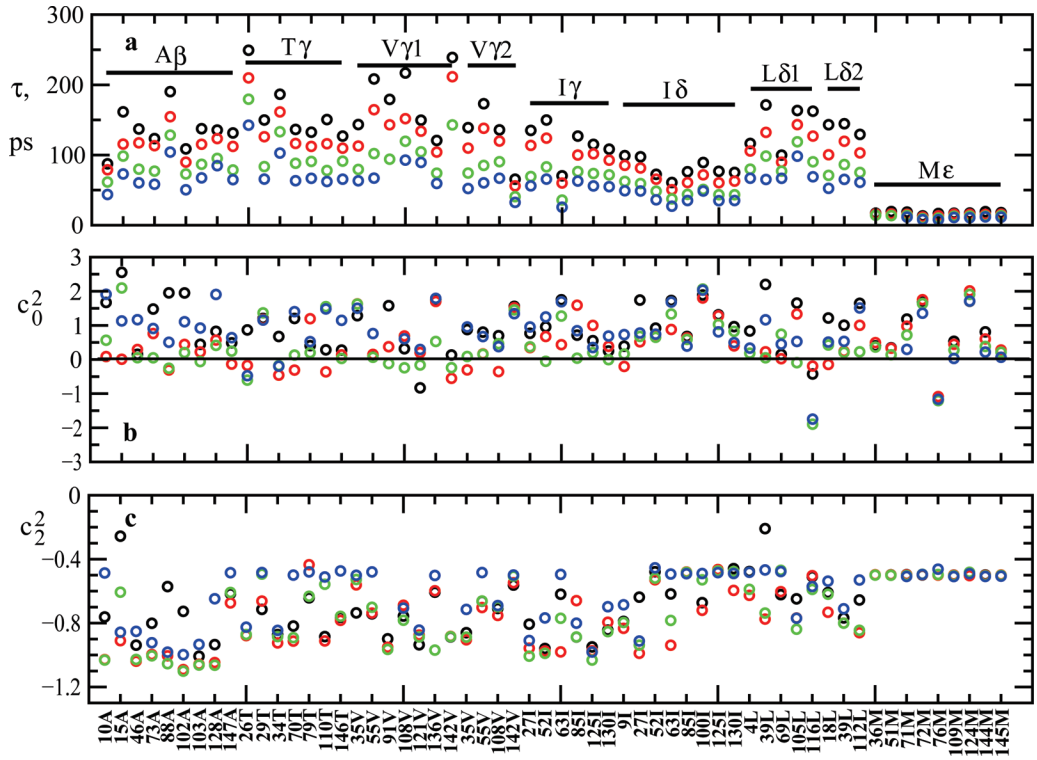

Figure 2. Best-fit local motional correlation time, τ (a), axial potential coefficient, c_0^2 (b), and rhombic potential coefficient, c_2^2 (c), as a function of methyl type at the various temperatures studied (black 288 K, red 299 K, green 308 K, blue 320 K). Details on the fitting procedure are given in the text.

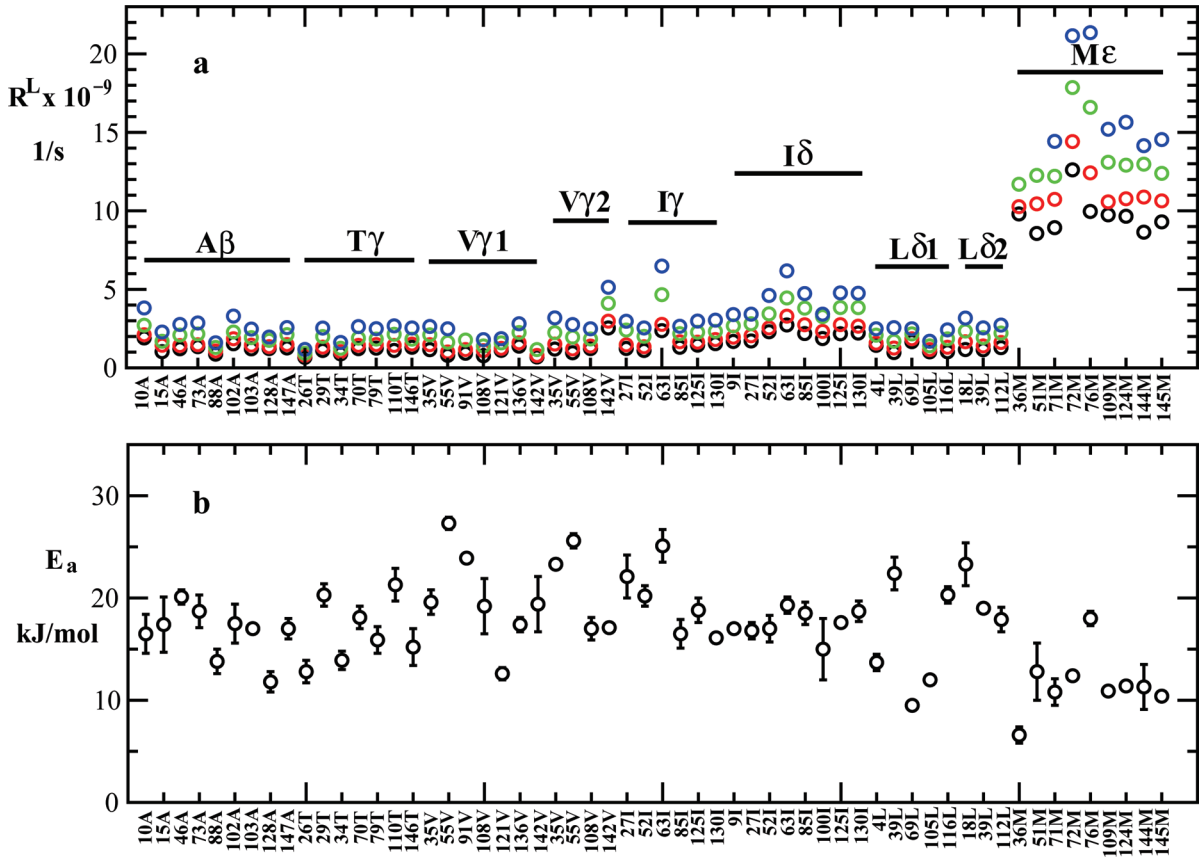

Figure 3. (a) Best-fit local motional rate, $R^L = 1/(6\tau)$, as a function of methyl type, at the various temperatures studied (black 288 K, red 299 K, green 308 K, blue 320 K). (b) Activation energies, E_a, as a function of methyl type, calculated with the Arrhenius equation from the R^L values shown in part a.

The alanine methyls exhibit the largest asymmetry, whereas the methionine methyls exhibit the smallest asymmetry.

Figure 6 shows the ordering tensor components S_0^2 and S_2^2 (eqs 3 and 4). The axial component, S_0^2, is mostly positive, in

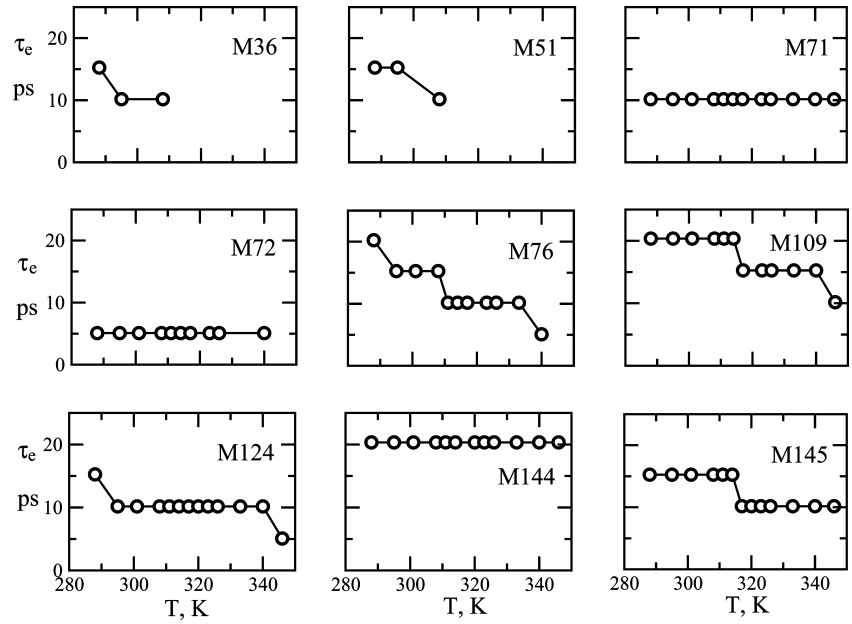

Figure 4. Effective local motional correlation time, τ_e MF, of the various methionine methyls of Ca^{2+}-CaM*smMLCKp as a function of temperature. The relevant experimental data from ref 20 were analyzed with the program Modelfree 4.0[41] adapted to methyl dynamics. Equation 7 was used; S_{axis}^2 and τ_e were allowed to vary.

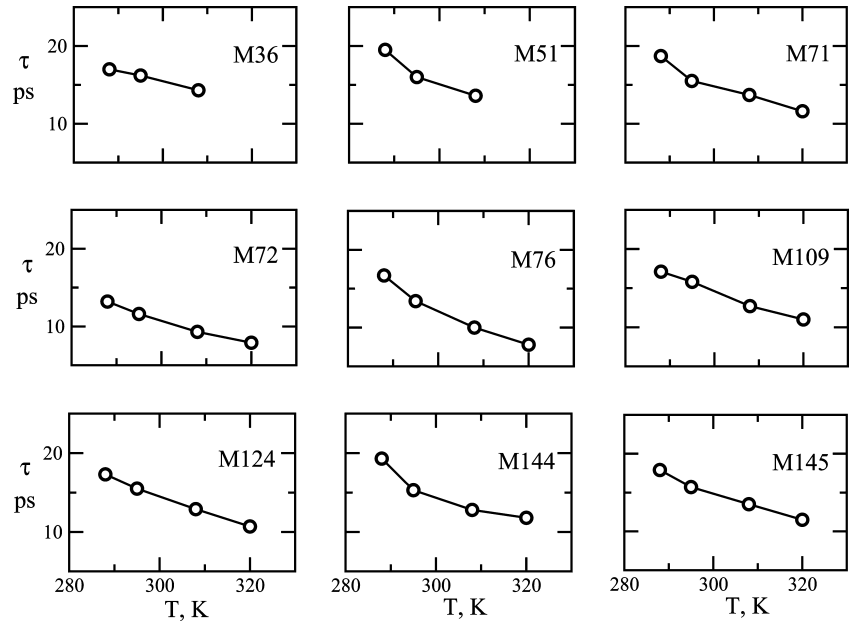

Figure 5. Local motional correlation time, $\tau = 1/(6R^L)$ SRLS, of the various methionine methyls of Ca^{2+}-CaM*smMLCKp as a function of temperature. The variables in these calculations were c_0^2, c_2^2, and R^L; β_{MQ} was allowed to depart from 110.5° by 1−2°.

some cases negative, and negative at all the temperatures studied for M76 and L$\delta_2$116. The rhombic component, S_2^2, is invariably negative. The data shown in Figures 2b,c reveal significant variations in the form of the POMT at the methyl sites of the complex Ca^{2+}-CaM*smMLCKp.

Average c_0^2 and c_2^2 values for all the methyl groups of Ca^{2+}-CaM*smMLCKp at the various temperatures studied are shown in Table 1. Between 288 and 308 K the parameter $\langle c_0^2 \rangle$ (the strength of the average POMT) decreases gradually, whereas $|\langle c_2^2 \rangle| \sim 0.7$. The ratio $|\langle c_2^2 \rangle / \langle c_0^2 \rangle|$ is a measure of potential rhombicity; this parameter increases gradually between 288 and 308 K. At 320 K the average POMT shows a sudden increase in $\langle c_0^2 \rangle$ and decrease in both $\langle c_2^2 \rangle$ and $|\langle c_2^2 \rangle / \langle c_0^2 \rangle|$. This might stem from the distinctively small temperature dependences of c_0^2 and c_2^2 for the methionine methyls (Figures 2b,c).

Table 1 also shows the average c_0^2 and c_2^2 values for alanine, methionine, and the other methyl types at 295 K. The potential forms are different for these three methyl types, as shown conspicuously by the corresponding data in Table 1. In Figure 7 we show the $|c_2^2|$ values obtained at 295 K as a function of methyl type. Values of $|c_2^2|$ of 1 and larger correspond exclusively to alanines, $|c_2^2|$ values of 0.5 and lower correspond exclusively to methionines, and in-between values correspond to all the other methyl types.

The alanine methyls are attached directly to the protein backbone. The local structure at the site of their motion is likely to be affected significantly by the structural properties of the backbone; there is experimental evidence for this.[42] It is thus reasonable that the POMT of the alanine methyls exhibits significant deviation from axiality, manifested as large $|c_2^2|$ values.

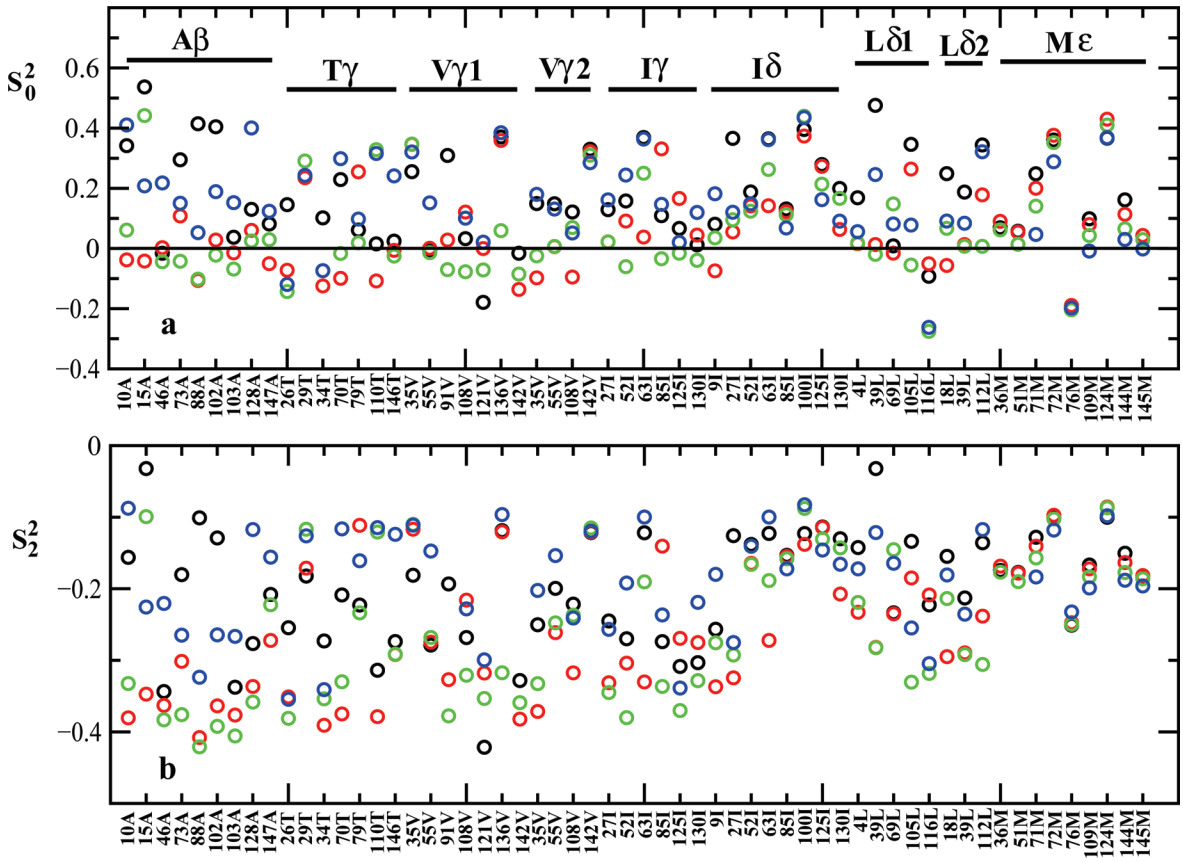

Figure 6. Axial S_0^2 (a) and rhombic S_2^2 (b) ordering tensor components, obtained from the best-fit potential coefficients c_0^2 and c_2^2 (cf. Figure 2b,c) using eqs 3 and 4, as a function of methyl type, at the various temperatures studied (black 288 K, red 299 K, green 308 K, blue 320 K). The variables in these calculations were c_0^2, c_2^2, and R^L; β_{MQ} was allowed to depart from 110.5° by 1−2°.

TABLE 1: Average c_0^2 and c_2^2 Values of the Methyl Groups of Ca^{2+}-CaM*smMLCKp as a Function of Temperature (Rows 1−4), and Average c_0^2 and c_2^2 Values for Alanines (A), Methionines (M), and All the Other Methyl Groups at 295 K (Rows 5−7)

	T, K	$\langle c_0^2 \rangle$	$\langle c_2^2 \rangle$	$\lvert\langle c_2^2 \rangle / \langle c_0^2 \rangle\rvert$
1	288	0.919	−0.676	0.74
2	295	0.471	−0.752	1.60
3	308	0.394	−0.735	1.87
4	320	0.792	−0.627	0.79
5	A (295 K)	0.216	−0.983	4.55
6	other (295 K)	0.489	−0.757	1.55
7	M (295 K)	0.645	−0.500	0.78

Four out of six threonine methyls also have large $|c_2^2|$ values (Figure 7), for similar reasons. The methionine methyls, S−CH_3, reside at the end of long side chains; they are well separated from the backbone, and partly hydrophilic due to the sulfur atom. Methionine methyls move significantly faster than all the other methyl types (Figure 3a). These observations are consistent with relative small deviation from axiality, i.e., small $|c_2^2|$ values (Figure 7), and relatively small variations in c_2^2 throughout the temperature range investigated (Figure 2c). The isoleucine δ methyls, which are also attached to relatively long side chains, have likewise small $|c_2^2|$ values (Figure 7) and fast local motional rates (Figure 3a). Thus, qualitative correlation between the magnitude of R^L and the asymmetry of the POMT on the one hand, and methyl type on the other hand, has been established effectively within the scope of the SRLS analysis.

It was reported that $S_{axis}{}^2$ values of Ca^{2+}-CaM*smMLCKp[32] (and other proteins[43]) cluster into three groups centered at the values of 0.2, 0.4, and 0.8. This has been interpreted as manifestation of the microscopic nature of entropy in proteins.[32] We show in Figure 7 the MF $S_{axis}{}^2$ values of the various methyl types of Ca^{2+}-CaM*smMLCKp, along with their $|c_2^2|$ values. It can be seen that $S_{axis}{}^2$ values on the order of 0.8, 0.2, and 0.4 are associated with different extents of nonaxiality of the POMT, which the SRLS analysis has correlated with alanines, methionines, and the other methyl types, respectively. The MF-based association is empirical in nature and does not connect with the methyl type. Correlation with entropic properties requires redefining S_{axis} ad hoc from the original expression of $\sqrt{(C^L(\infty))}$/0.1, to the physical expression of eq 4.[32] In addition, one has to guess the form of $u(\Omega_{CM})$ in the Boltzmann factor that enters eq 4. The SRLS-based rationalization is straightforward within the scope of a general stochastic model for treating methyl dynamics.

3.2. Typical POMTs and Associated Relative Probability Distributions. We show in Figure 8a,c the local potentials, $u(\Omega_{CM})$ (cf. eq 3), obtained at 295 K for the methyl groups A10 and Iδ85, plotted as a function of the angles β_{CM} and γ_{CM} in radians. Note that u is the actual potential, U, divided by k_BT, rendering u dimensionless. Figure 8b,d shows the corresponding relative (or unnormalized) probability distribution function, $P_{rel} = \exp(-u)\sin\beta_{CM}\Delta\beta_{CM}\Delta\gamma_{CM}$. P_{rel} is the probability of the main local ordering axis having an orientation in the infinitesimal ranges $\beta_{CM} \pm \Delta\beta_{CM}$ and $\gamma_{CM} \pm \Delta\gamma_{CM}$ for any α_{CM} (since the C frame is uniaxial).[44] Representations of the functions $P_{rel}(\beta_{CM},\gamma_{CM})$ are obtained by plotting $Z_C = R\cos\beta_{CM}$ vs $X_C = R\sin\beta_{CM}\cos\gamma_{CM}$ and $Y_C = R\sin\beta_{CM}\sin\gamma_{CM}$, where $R = \exp(-u)\sin\beta_{CM}$.

The best-fit parameters, obtained with the data fitting strategy outlined above, are $c_0^2 = 0.087$, $c_2^2 = -1.089$, $\beta_{MQ} = 112°$, and

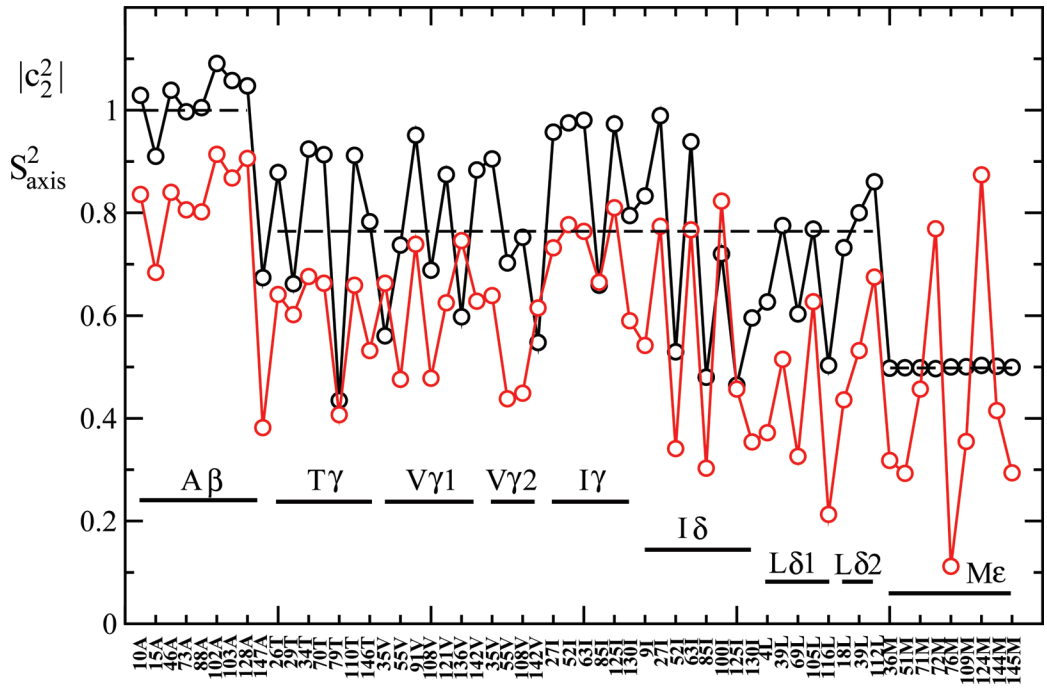

Figure 7. $|c_2^2|$ from Figure 2c (black circles) and the corresponding S_{axis}^2 value from ref 20 (red circles) as a function of methyl type, at 295 K. The dashed lines represent the absolute values of $\langle c_2^2 \rangle$ given in Table 1 for the alanine, "other" and methionine methyl groups.

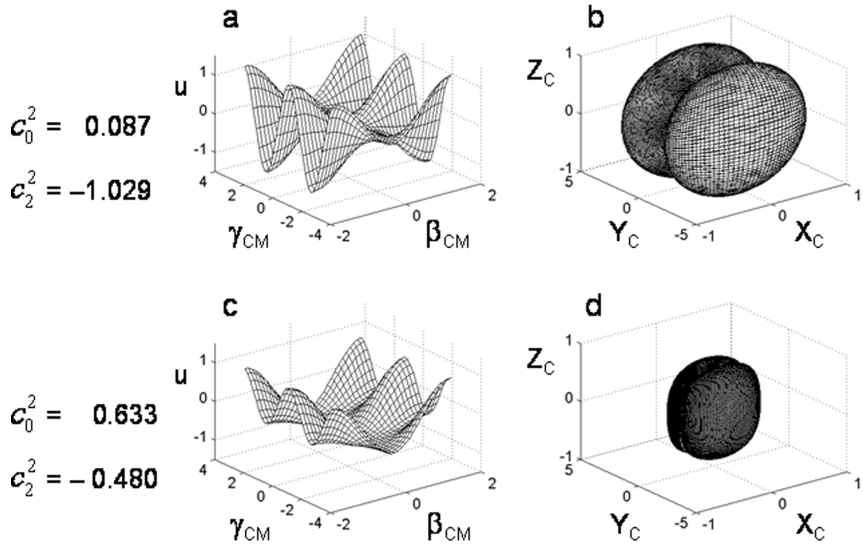

Figure 8. (a) Potential $u = -0.087 \times (3/2 \cos^2 \beta_{CM} - 1/2) + 1.089 \times (3/2)^{1/2} \sin^2 \beta_{CM} \cos 2\gamma_{CM}$ as a function of β_{CM} and γ_{CM} given in radians. The potential coefficients are the best-fit values obtained by fitting with SRLS the experimental data of methyl group A10 of Ca^{2+}-CaM*smMLCKp, as described in the text. (b) The relative probability P_{rel} of the C−$^{13}CDH_2$ axis having an orientation in the infinitesimal range $\beta_{CM} \pm \Delta\beta_{CM}$ and $\gamma_{CM} \pm \Delta\gamma_{CM}$, for any α, given by $\exp[0.087 \times (3/2 \cos^2 \beta_{CM} - 1/2) - 1.089 \times (3/2)^{1/2} \sin^2 \beta_{CM} \cos 2\gamma_{CM}]\sin \beta_{CM}\Delta\beta_{CM}\Delta\gamma_{CM}$, as a function of the spherical coordinates (β_{CM},γ_{CM}). In this context, the uniaxial local director is defined to lie along the equilibrium C−$^{13}CDH_2$ orientation. (c) The potential $u = -0.633 \times (3/2 \cos^2 \beta_{CM} - 1/2) + 0.480 \times (3/2)^{1/2} \sin^2 \beta_{CM} \cos 2\gamma_{CM}$ as a function of β_{CM} and γ_{CM} given in radians. The potential coefficients are the best-fit values obtained by fitting with SRLS the experimental data of methyl group Iδ85 of Ca^{2+}-CaM*smMLCKp (see text for details). (d) The relative probability of the C−$^{13}CDH_2$ axis having an orientation in the infinitesimal range $\beta_{CM} \pm \Delta\beta_{CM}$ and $\gamma_{CM} \pm \Delta\gamma_{CM}$, for any α, given by $\exp[0.633 \times (3/2 \cos^2 \beta_{CM} - 1/2) - 0.480 \times (3/2)^{1/2} \sin^2 \beta_{CM} \cos 2\gamma_{CM}]\sin \beta_{CM}\Delta\beta_{CM}\Delta\gamma_{CM}$, as a function of the spherical coordinates (β_{CM},γ_{CM}).

$\tau/\tau_m = 0.0067$ for A10, and $c_0^2 = 0.633$, $c_2^2 = -0.480$, $\beta_{MQ} = 113°$, and $\tau/\tau_m = 0.0051$ for Iδ85. The rhombic potential prevailing at the site of the motion of the methyl A10 is shown in Figure 8a. Its rhombicity, $|c_2^2/c_0^2|$, is equal to 12.6; this represents very large asymmetry. The Cartesian ordering tensor components calculated in terms of this potential, shown in Table 2, indicate that "Y-ordering" prevails at this methyl site. The shape of the corresponding P_{rel} function, shown in Figure 8b, bears out this symmetry.

TABLE 2: Potential Coefficients, c_0^2 and c_2^2, Obtained with SRLS-Based Fitting of the Experimental ^2H T_1 and T_2 Relaxation Parameters of the Methyl Groups A10 and Iδ85 of Ca^{2+}-CaM*smMLCKp[a]

methyl group	c_0^2	c_2^2	S_{xx}	S_{yy}	S_{zz}
A10	0.087	−1.089	−0.214	0.252	−0.038
Iδ85	0.633	−0.480	−0.156	0.034	0.122

[a] The order parameters S_{xx}, S_{yy}, and S_{zz} were calculated from c_0^2 and c_2^2 as outlined in the text.

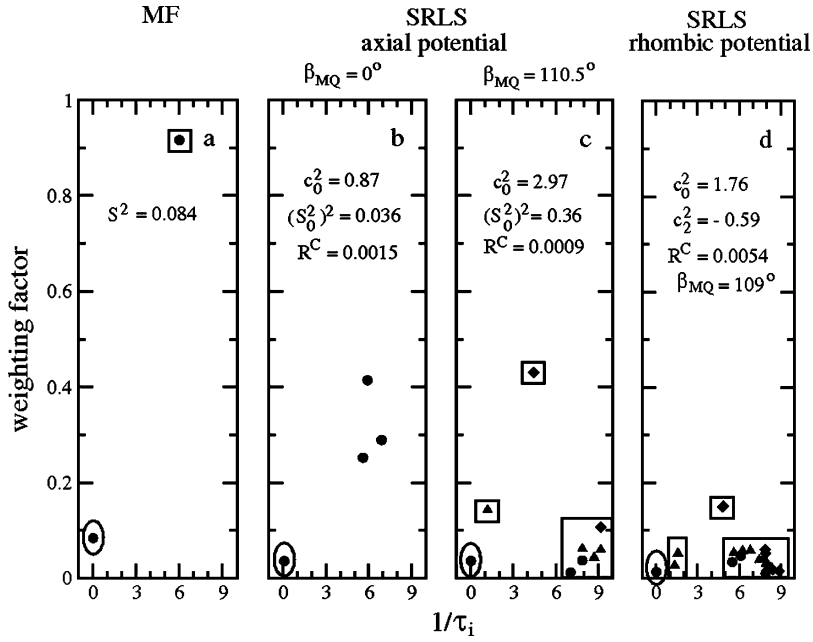

Figure 9. SRLS weighting factors of the eigenmodes (ordinate) and corresponding eigenvalues (abscissa) of $C_{00}(t)$ (circles), $C_{11}(t)$ (triangles), and $C_{22}(t)$ (diamonds). The unitless eigenvalue, $1/\tau_i$, is given in units of the local motional rate, R^L. The unitless parameter R^C represents the time scale separation, τ/τ_m. The parameters within the panels (except for the S_0^2 values which were calculated from corresponding c_0^2 values) are best-fit values obtained by analyzing with SRLS-based fitting (Figure 9b−d) or MF-based fitting (Figure 9a) the experimental ^{2}H R_1 and R_2 data[20] of methyl group A10 of Ca^{2+}-CaM*smMLCKp, acquired at 14.1 and 17.6 T, and 295 K. The parameters on the top were fixed in the respective data fitting calculation. The various panels correspond to different parameter combinations used. The boxes mark clusters of eigenvalues comparable in magnitude.

The rhombic potential prevailing at the site of the motion of the methyl Iδ85 is shown in Figure 8c. The $|c_2^2/c_0^2|$ ratio is 0.76, indicating smaller asymmetry of the local potential as compared to methyl A10. The Cartesian tensor components given in Table 2 indicate that "nearly planar X−Z ordering" prevails at this methyl site. The shape of the corresponding P_{rel} function, shown in Figure 8d, bears out this symmetry.

In Figure 1b, we illustrate "X-ordering". The SRLS analysis presented in this study shows that this is just an example. The POMT at methyl sites is sensitive to the combined effect of methyl type and local structure; it has to be determined for each case by data fitting. It will be interesting and useful to correlate the SRLS POMT, $u(\Omega_{CM})$, and the associated ordering tensor, $\boldsymbol{S}$, with both experimentally determined (with X-ray crystallography or NMR), and MD-simulated, protein structures.

The MF analysis yielded $S_{axis}{}^2 = 0.84$ for A10 and $S_{axis}{}^2 = 0.303$ for Iδ85 at 295 K.[20] Thus, according to MF the C−CH_3 bond of A10 is highly ordered; this is expected. On the other hand, the C−CH_3 bond of Iδ85 is involved in large-amplitude axial fluctuations. This is incompatible with the local stereochemistry and the packing properties of protein cores. According to SRLS the A10 and Iδ85 methyl groups, and in general all the methyl groups in Ca^{2+}-CaM*smMLCKp, reorient in the presence of weak rhombic local potentials. Different methyl groups experience different potential forms determined by their type, and the structure of their immediate surroundings.

3.3. Eigenmodes. The SRLS time correlation functions comprise sums of weighted exponents. The decay constants are the eigenvalues of the SRLS time evolution operator Γ; we denote them egv. The corresponding eigenvectors are the eigenmodes; we denote their respective weighting factors egm. In the following, we characterize TCF functions in terms of the significantly contributing egv/egm terms.

In its physical connotation, where $S^2 = (S_0^2)^2$ and $\tau_e = \tau = 1/(6R^L)$, the MF spectral density of eq 6 can be described as follows. The local motional eigenvalue is $egv^L = 6$ (in units of R^L) and its weighting factor is $egm^L = (1 - S^2)$; the global motional eigenvalue is $egv^G = (\tau_e/\tau_m) \times 6$ and its weighting factor is $egm^G = S^2$. The labels "G" and "L" indicate that the Wigner functions of the "bare" degrees of freedom have been preserved. The fact that $egm^G = S^2$ (and perforce $egm^L = (1 - S^2)$) is implied by considering S^2 to be the same as $(S_0^2)^2$.

The data set comprising ^{2}H T_1 and T_2 of the methyl A10, acquired at 14.1 and 17.6 T, 295 K, is used as an example. MF analysis based on eq 6 yields $S^2 = 0.084$ and $\tau_e = 77$ ps (calculated by us with Modelfree 4.0[41] adapted to methyl dynamics) as best-fit parameters, with $\tau_m = 11.81$ ns from ref 20. The egv/egm contributions are $egv^G/egm^G = 0.039$ (0.084) and $egv^L/egm^L = 6$ (0.916). Figure 9a shows the eigenmode weighting factors on the ordinate and the eigenvalues on the abscissa.

In the corresponding SRLS calculation we allowed c_0^2 and R^C to vary, fixing $\beta_{MQ} = 0$ and $c_2^2 = 0$. The parameter c_0^2 yields $(S_0^2)^2$, which is formally analogous to S^2, and R^C is the formal analogue of τ_e/τ_m. The best-fit parameters are $c_0^2 = 0.87$ (which yields $(S_0^2)^2 = 0.036$) and $R^C = 0.0015$. These values were used as input to the calculation of $C(t) = C_{00}(t)$ (only the $K,K' = 0,0$ component contributes to $C(t)$ when $\beta_{MQ} = 0$). The egv (egm) contributions are 0.0355 (0.0376), 5.96 (0.350), 5.63 (0.5), and 6.93 (0.094). The total fractional contribution is 0.9906 (we ignore the large number of eigenvalues with very small weighting factors, which contribute the 0.0094 fraction). Figure 9b shows the contributing eigenmode weighting factors and their corresponding eigenvalues. We also show these data, along with the egv/egm contributions to the $C_{11}(t)$ and $C_{22}(t)$ functions associated with this calculation, in Table 3, to enable comparison with subsequent scenarios where the $K,K' = 1,1$ and 2,2 components also contribute.

In the large time scale separation, which holds true for methyl dynamics, the SRLS pair 0.0355 (0.0376) represents within a good approximation the global motion. Hence one may compare it with 0.039 (0.084) in MF. The MF parameter S^2 has the value

TABLE 3: Dominant Weighting Factors of the Eigenmodes, $c_{K,K',i}$ and Corresponding Eigenvalues, $1/\tau_i$, Comprising $C_{00}(t)$, $C_{11}(t)$, and $C_{22}(t)$, Calculated with $c_0^2 = 0.87$, $c_2^2 = 0$, $\beta_{MQ} = 0°$, and $R^C = 0.0015$[a]

$C_{00}(t)$		$C_{11}(t)$		$C_{22}(t)$	
$1/\tau_i$	$c_{00,i}$	$1/\tau_i$	$c_{11,i}$	$1/\tau_i$	$c_{22,i}$
5.96	0.350	5.96	0.330	5.34	0.527
5.63	0.328	6.22	0.302	6.57	0.374
5.63	0.181	6.54	0.292	6.98	0.096
6.93	0.094	1.73	0.069		
0.0355	0.0376				
1.0	0.0			0.0	
MF[20]					
6	0.916				
N.A.	0.084				

[a] The values of c_0^2 and R^C are best-fit parameters obtained with SRLS-based fitting of the ^2H T_1 and T_2 data from the A10 methyl of Ca^{2+}-CaM*smMLCKp acquired at 14.1 and 17.6 T, and 295 K. The experimental data and $\tau_m = 11.81$ ns were taken from ref 20. The fractional contributions of the $j_{KK}(\omega)$ functions to $J^{QQ}(\omega)$, and the MF data from ref 20 obtained with eq 2, are also shown. The eigenvalues, $1/\tau_i$, are given in units of R^L.

of 0.084 whereas the SRLS parameter $(S_0^2)^2$ has the value of 0.0376. The time scale separation is $\tau_e/\tau_m = 0.0065$ in MF and $\tau/\tau_m = 0.0059$ in SRLS. Thus, even though the time scale separations are large, and the axial local ordering and magnetic frames are collinear in both calculations, the squared order parameter (the local motional correlation time) is 2.2 (1.1) times larger in MF in comparison with SRLS. The large discrepancy between the order parameters is implied by the fact that the Wigner functions are no longer eigenfunctions of the local motional diffusion operator in the presence of a POMT given by $c_0^2 = 0.87$. This is ignored in MF, where a single decay constant for the local motion, $1/\tau_e$, representing a Wigner function scenario, is assumed allegedly. The more physically meaningful SRLS calculation shows that three main local motional eigenmodes with eigenvalues 5.96, 5.63, and 6.93, and corresponding weighting factors of 0.350, 0.5, and 0.094, are present.

We proceed by accounting for the local geometry. This is done in MF implicitly through the coefficient 0.1 featured by eq 7. This spectral density, which is a recasting of eq 6, comprises $egv^G/egm^G = 0.039$ (0.84) and $egv^L/egm^L = 6$ (0.16). In the corresponding SRLS calculation, we allowed c_0^2 and R^C to vary, fixing $\beta_{MQ} = 110.5°$ and $c_2^2 = 0$. We obtained $c_0^2 = 2.97$ (which yields $(S^2_0)^2 = 0.36$) and $R^C = 0.0009$ as best-fit values. The latter were used as input to the calculation of $C_{00}(t)$, $C_{11}(t)$, and $C_{22}(t)$ (which are the relevant TCFs when the (axial) M and Q frames are tilted). The coefficients of these functions in the measurable TCF are 0.1, 0.323, and 0.577 (cf. eq 10); hence, the weighting factors are scaled when they enter the measurable time correlation function (or spectral density).

Table 4 features the unscaled weighting factors; the scaled weighting factors are shown in Figure 9c by circles, triangles and diamonds for the $C_{00}(t)$, $C_{11}(t)$, and $C_{22}(t)$ contributions, respectively. Parts c and b of Figure 9 differ significantly. Clearly, the $\beta_{MQ} = 110.5°$ geometry, hence Figure 9c, is correct. However, the results illustrated in Figure 9c are not acceptable because $c_0^2 = 2.97$ represents a *weak axial* POMT, which, as pointed out above, is not considered to be appropriate from a physical point of view.

SRLS analyses of methyl dynamics based on axial potentials yielded results with several problematic aspects.[28,29] Many of these matters could be resolved by allowing for rhombic

TABLE 4: Dominant Weighting Factors of the Eigenmodes, $c_{KK',i}$, and Corresponding Eigenvalues, $1/\tau_i$, Comprising the Time Correlation Functions $C_{00}(t)$, $C_{11}(t)$, and $C_{22}(t)$, Calculated with $c_0^2 = 2.97$, $c_2^2 = 0$, $\beta_{MQ} = 110.5°$, and $R^C = 0.0009$[a]

$C_{00}(t)$		$C_{11}(t)$		$C_{22}(t)$	
$1/\tau_i$	$c_{00,i}$	$1/\tau_i$	$c_{11,i}$	$1/\tau_i$	$c_{22,i}$
7.65	0.378	1.21	0.419	4.47	0.735
0.006	0.329	7.65	0.193	8.94	0.193
6.93	0.130	8.93	0.190	10.1	0.045
		8.46	0.145		
0.1		0.323		0.577	

[a] The values of c_0^2 and R^C are the best-fit parameters obtained with SRLS-based fitting of the same experimental data as outlined in the title of Table 3. The fractional contributions of the corresponding $j_{KK}(\omega)$ functions to $J^{QQ}(\omega)$ are also shown. The eigenvalues, $1/\tau_i$, are given in units of R^L.

potentials.[28,29] We therefore proceed by subjecting the experimental data of A10 to SRLS analysis where rhombic potentials are allowed for. For meaningful comparion with the axial potentials considered so far, we use results that feature "Z-ordering" and have the angle β_{MQ} closest to 110.5°. The corresponding best-fit values are $c_0^2 = 1.76$, $c_2^2 = -0.59$, $R^C = 0.0054$, and $\beta_{MQ} = 109°$. These values have been used as input to the calculation of the $C_{KK'}(t)$ functions for $K,K' = 0,0$; 1,1; 2,2; 2,0; 1,−1, and 2,−2 (cf. eq 5). The corresponding scaling factors to be applied to the weighting factors of the eigenmodes are 0.14, 0.354, 0.474, −0.095, 0.045, and 0.082. The scaled weighting factors of the eigenmodes contributed by $C_{00}(t)$, $C_{11}(t)$, and $C_{22}(t)$ are depicted in Figure 9d; the unscaled values are shown in Table 5.

Figure 9d differs significantly from Figure 9c. The calculation illustrated in Figure 9d, featuring a rhombic potential, is appropriate both from a physical point of view and from a statistical point of view (low χ^2); hence, it is accepted. There is ample evidence for nonaxial restrictions underlying methyl dynamics in proteins.[26−28,45−47]

Further insight into the effect of mode-coupling, general features of local geometry, and tensor symmetry can be gained by careful comparison of corresponding data shown in Tables 3−5. As expected, mode-coupling has a small effect in methyl dynamics because the local motion of the methyl group is much faster than the global tumbling of the protein. On the other hand, as a result of a POMT which is rhombic, the solution of the Smoluchowski equation is no longer analytical, but rather yields multiexponantial decaying time correlation functions.

The version of eq 6 in which $S^2 = (S_0^2)^2$ and $\tau_e = \tau = 1/(6R^L)$ constitutes the simplest physically sound description of the two-body problem.[48] Equation 7 is a reformulation of eq 6. It cannot possibly represent a three-body problem with the two local motions necessarily related geometrically, but with no provision to account for geometric features, unless one resorts to the utilization of constructs (τ_e and $S_{axis}{}^2$). The results are impaired thereby;[27,28] even trends may be misleading. For example, $(S_0^2)^2 = 0.36$ whereas $S_{axis}{}^2 = 0.84$ for methyl A10, and $(S_0^2)^2 = 0.14$ whereas $S_{axis}{}^2 = 0.11$ for methyl M76. The parametrizing values, $S_{axis}{}^2$, span a significantly larger range than the physical values, $(S_0^2)^2$;[18] the relation between $(S_0^2)^2$ and $S_{axis}{}^2$ is not linear.[29] Therefore, care is to be exerted in using $S_{axis}{}^2$ and τ_e to derive information considered biologically relevant.[49−53]

3.4. Aspects of Structural and Functional Dynamics. ***Structural Features.*** SRLS provides both the axial, S_0^2, and rhombic, S_2^2, order parameters (Figure 6; see above). The

TABLE 5: Dominant Weighting Factors of the Eigenmodes, $c_{KK',i}$, and Corresponding Eigenvalues, $1/\tau_i$, Comprising the Time Correlation Functions $C_{00}(t)$, $C_{11}(t)$, and $C_{22}(t)$ Calculated with $c_0^2 = 1.76$, $c_2^2 = -0.59$, $\beta_{MQ} = 109.5°$, and $R^C = 0.054$[a]

$C_{00}(t)$		$C_{11}(t)$		$C_{22}(t)$	
$1/\tau_i$	$c_{00,i}$	$1/\tau_i$	$c_{11,i}$	$1/\tau_i$	$c_{22,i}$
5.81	0.317	6.24	0.187	5.12	0.280
5.20	0.265	5.85	0.182	4.90	0.274
7.74	0.201	5.23	0.164	7.92	0.134
0.042	0.079	1.82	0.122	7.90	0.109
7.90	0.064	7.61	0.118	2.93	0.05
4.90	0.041	7.65	0.109	5.81	0.04
8.93	0.013	8.00	0.07	8.22	0.03
		1.37	0.03	8.93	0.03
				5.20	0.03

$C_{02}(t)$		$C_{1-1}(t)$		$C_{2-2}(t)$	
$1/\tau_i$	$c_{02,i}$	$1/\tau_i$	$c_{1-1,i}$	$1/\tau_i$	$c_{2-2,i}$
5.81	0.286	5.85	0.363	4.90	0.546
5.20	0.232	5.23	0.328	7.90	0.218
7.74	0.148	7.61	0.237	5.81	0.075
5.12	0.137	1.37	0.057	8.93	0.056
7.92	0.07			5.20	0.056
4.90	0.05			7.74	0.019
2.93	0.025			0.042	0.018
0.042	0.017				
8.22	0.015				

KK'	0,0	1,1	2,2	0,2	1,−1	2,−2
	0.14	0.35	0.47	−0.1	0.05	0.08

[a] The values of c_0^2, c_2^2, β_{MQ}, and R^C are the best-fit parameters obtained with SRLS-based fitting of the same experimental data as outlined in the title of Table 3. The fractional contributions of the corresponding $j_{KK}(\omega)$ functions to $J^{QQ}(\omega)$ are also shown. The eigenvalues, $1/\tau_i$, are given in units of R^L.

absolute values of S_0^2 and S_2^2 are small and comparable in magnitude. This signifies weak and highly rhombic local ordering. Different relative signs of S_0^2 and S_2^2 correspond to different rhombic symmetries. The same kind of information can be derived from the coefficients of the local potential, c_0^2 and c_2^2 (Figure 2b,c). The orientation of the local ordering frame relative to the magnetic quadrupolar frame is given by the angle β_{MQ}, which is within 1−2° from 110.5°. This means that the main local ordering axis is nearly parallel to the C−CH_3 bond.

The structural information outlined above is mesoscopic in nature. Establishing correlations at the atom level between the SRLS parameters S_0^2, S_2^2, and E_a, and structural features of the Ca^{2+}-calmodulin*smMLCKp complex has to await the development of appropriate integrated methodologies which combine mesoscopic and atomistic approaches. Such developments exist in different contexts;[54−63] adaptation to NMR spin relaxation in proteins is in progress.

Molecular Dynamics. The Ca^{2+}-calmodulin*smMLCKp complex was studied with MD simulations.[64] Squared generalized order parameters, S^2(MD), were calculated with a simple formula applicable to ultrafast local motions.[65] As typically found,[37,66,67] the parameter S^2(MD) overestimates S^2(MF). This is likely associated with different parametrization of the actual time correlation function in the MF and MD analyses.[19] The only correlation established between S^2(MD) and the 3D structure of Ca^{2+}-calmodulin*smMLCKp is the proximity of the side chains of aromatic residues to a given methyl group.[64]

The alanine methyl groups of staphylococcal nuclease were investigated.[40] It was found that infrequently sampled low-barrier conformations might affect the results significantly. Integrated approaches might be useful in this context.

Xue et al. studied methyl dynamics in the SH3 domain of α-spectrin with both ^{2}H NMR relaxation analyzed with MF, and with MD.[30] The MF analysis yielded an average barrier height of 2.8 kcal/mol. The MD simulations yielded average barrier heights of 3.1−3.5 kcal/mol. The analysis of several NMR structures from the Protein Data Base yielded average barrier heights of 4−6 kcal/mol.

Currently comparisons are made between results from MF analyses of the NMR data and MD.[30,37,40,45,67] We argue in this article that the results of a SRLS analysis are more physically relevant than those from MF, so it would be appropriate to make comparisons between SRLS and MD. Once the SRLS analysis is completed, producing the best-fit values of the parameters which define the local potentials, the diffusion tensors, and the geometric factors (i.e., the relative frame orientations), relevant time correlation functions of the $D^2_{MK}(\Omega)$ can readily be computed. It would be then of interest to calculate the equivalent time correlation functions from the MD trajectories and compare with their SRLS counterparts.[19] Such comparisons, carried out as desribed, or eventually within the scope of integrated approaches,[54−63] might provide new insights.

Biological Function. The effect of Ca^{2+} binding on the side-chain methyl dynamics of calbindin D_{9k} was studied.[49] The results revealed correlation between a methyl group's distance from the Ca^{2+} binding site and its conformational dynamics. Two classes, one proximal and the other one distal, were identified according to the values of the best-fit MF parameters. It was inferred that the distal and proximal methyl groups respond differently to Ca^{2+} binding. A new trend, exhibited by the distal methyl groups, was linked to an important mechanism by which calbindin D_{9k} achieves high affinity binding while minimizing the corresponding loss of conformational entropy. The term "polar dynamics" was introduced.

Information on ligand-dependent dynamics and intramolecular signaling was obtained by analyzing with MF ^{2}H methyl relaxation in a PDZ domain.[50] This line of reasoning was pursued to suggest that position 20 in the human tyrosine phosphatase 1E protein acts as a critical "hub" for transmitting changes in dynamics.[51] Side-chain methyl MF order parameters have been used to infer on hidden dynamic allostery in a PDZ domain.[52]

Since the absolute values of the MF parameters and the variations therein are inaccurate, the biologically relevant assessments mentioned above might change upon SRLS analysis of the same experimental data.

Conformational Entropy. The parameter S_{axis} has been used to derive conformational entropy in the context of ligand binding or temperature variations.[6,32] As pointed out above, the accuracy of S_{axis}, and its physical meaning, are problematic. An axial potential, with an ad hoc defined shape, is calculated from S_{axis} and used further to calculate conformational entropy. In SRLS conformational entropy is calculated directly from the rhombic potential determined by physical data fitting. Since this potential is significantly more realistic than the axial MF potentials mentioned above, the SRLS-based entropy is more accurate and informative than the MF-based entropy. Information associated with the Ca^{2+}-calmodulin*smMLCKp complex appears in ref 19. We found that the variations in the experimental data are associated primarily with variations in the rhombicity of the local spatial restrictions represented by either S_2^2 or c_2^2.[19] The overall picture provided by SRLS differs significantly from the overall picture provided by MF.

4. Conclusions

Local motional rates and associated activation energies are reported for all the experimentally studied methyl groups of Ca^{2+}-CaM*smMLCKp. In the temperature range of 288−320 K the local motional rates lie in the range 8.6×10^9 to 21.4×10^9 1/s for methionines, and 0.67×10^9 to 6.5×10^9 1/s for all the other methyl types. The activation energies for local motion are approximately 10 kJ/mol for methionines, and 10−27 kJ/mol for all the other methyl types. The potential of mean torque is weak and nonaxial; its form differs for alanines, methionines, and all the other methyl types. The measurable time correlation function represents predominantly the local motion. It comprises a relatively large number of eigenmodes resulting from the POMT, and its rhombic symmetry. The spectral density used in model-free analyses of methyl dynamics in proteins is physically vague; so are the parameters that enter it. The three classes of S_{axis}^2 associated in the literature with the microscopic origin of the entropy in proteins are shown to be associated with different forms of the POMT. Both the activation energies and the POMT forms represent important information because they relate to the local structure. Well-defined physical rates for local methyl motion provide important kinetic information.

Acknowledgment. This work was supported by the Israel Science Foundation (Grant No. 347/07 to E.M.), the Binational Science Foundation (Grant No. 2006050 to E.M. and J.H.F.), the German-Israeli Science Foundation for Scientific Research and Development, grant no. 928-190.0/2006, and the Damadian Center for Magnetic Resonance at Bar-Ilan University, Israel. This work was also supported by the National Center for Research Resources of the National Institutes of Health (Grant No. P41-RR016292 to J.H.F.). A.P. acknowledges support provided by Ministero dell'Istruzione, Universita e Ricerca (MIUR), grant PRIN 2008 and by the University of Padova, grant "Progetto Strategico" HELIOS 2009. E.M. gratefully acknowledges the hospitality of the Department of Computational and Systems Biology, University of Pittsburgh School of Medicine, where she spent her sabbatical year 2009/2010, in the course of which this work was finalized.

Abbreviations. Ca^{2+}-CaM, Ca^{2+}−calmodulin; EMF, extended model free; MD, molecular dynamics; MF, model-free; NMR, nuclear magnetic resonance; NOE, nuclear Overhauser enhancement; POMT, potentital of mean torque; SRLS, slowly relaxing local structure; TCF, time correlation function.

References and Notes

(1) Ishima, R.; Torchia, D. A. *Nat. Struct. Biol.* **2000**, *7*, 740.
(2) Case, D. A. *Acc. Chem. Res.* **2002**, *35*, 325.
(3) Brüschweiler, R. *Curr. Opin. Struct. Biol.* **2003**, *13*, 175.
(4) Palmer, A. G. *Chem. Rev.* **2004**, *104*, 3623.
(5) Mittermaier, A.; Kay, L. E. *Science* **2006**, *312*, 224.
(6) Igumenova, T. I.; Frederick, K. K.; Wand, A. J. *Chem. Rev.* **2006**, *106*, 1672.
(7) Kitao, A.; Wagner, G. *Magn. Reson. Chem.* **2006**, *44*, S130.
(8) Jarymowycz, V. A.; Stone, M. J. *Chem. Rev.* **2006**, *106*, 1624.
(9) Nodet, G.; Abergel, D. *Eur. Biophys. J. Biophys. Lett.* **2007**, *36*, 985.
(10) Markwick, P. R. L.; Malliavin, T.; Nilges, M. *PLoS Comput. Biol.* **2008**, *4*, 1.
(11) Muhandiram, D. R.; Yamazaki, T.; Sykes, B. D.; Kay, L. E. *J. Am. Chem. Soc.* **1995**, *117*, 11536.
(12) Millet, O.; Muhandiram, D. R.; Skrynnikov, N. R.; Kay, L. E. *J. Am. Chem. Soc.* **2002**, *124*, 6439.
(13) Srynnikov, N. R.; Millet, O.; Kay, L. E. *J. Am. Chem. Soc.* **2002**, *124*, 6449.
(14) Polimeno, A.; Freed, J. H. *Adv. Chem. Phys.* **1993**, *83*, 89.
(15) Polimeno, A.; Freed, J. H. *J. Phys. Chem.* **1995**, *99*, 10995.
(16) Liang, Z.; Freed, J. H. *J. Phys. Chem. B* **1999**, *103*, 6384.
(17) Tugarinov, V.; Liang, Z.; Shapiro, Yu. E.; Freed, J. H.; Meirovitch, E. *J. Am. Chem. Soc.* **2001**, *123*, 3055.
(18) Meirovitch, E.; Shapiro, Yu. E.; Polimeno, A.; Freed, J. H. *J. Phys. Chem. A* **2006**, *110*, 8366.
(19) Meirovitch, E.; Shapiro, Yu. E.; Polimeno, A.; Freed, J. H. *Prog. NMR Spectrosc.* **2010**, *56*, 360.
(20) Lee, A.; Sharp, K. A.; Kranz, J. K.; Song, X.-J.; Wand, A. J. *Biochemistry* **2002**, *41*, 13814.
(21) Kay, L. E.; Torchia, D. A.; Bax, A. *Biochemistry* **1989**, *28*, 8972.
(22) Lipari, G.; Szabo, A. *J. Am. Chem. Soc.* **1982**, *104*, 4546.
(23) Lipari, G.; Szabo, A. *J. Am. Chem. Soc.* **1982**, *104*, 4559.
(24) Clore, G. M.; Szabo, A.; Bax, A.; Kay, L. E.; Driscoll, P. C.; Gronenborn, A. M. *J. Am. Chem. Soc.* **1990**, *112*, 4989.
(25) Woessner, D. E. *J. Chem. Phys.* **1962**, *36*, 1.
(26) Avitabile, J.; London, R. E. *J. Am. Chem. Soc.* **1978**, *100*, 7159.
(27) Tugarinov, V.; Kay, L. E. *J. Biomol. NMR* **2004**, *29*, 369.
(28) Meirovitch, E.; Polimeno, A.; Freed, J. H. *J. Phys. Chem. B* **2006**, *110*, 20615.
(29) Meirovitch, E.; Shapiro, Yu. E.; Polimeno, A.; Freed, J. H. *J. Phys. Chem. B* **2007**, *111*, 12865.
(30) Xue, Y.; Pavlova, M. S.; Ryabov, Y. E.; Reif, B.; Skrynnikov, N. R. *J. Am. Chem. Soc.* **2007**, *129*, 6827.
(31) Emsley, J. W.; Luckhurst, G. R.; Stockley, C. P. *Proc. R. Soc. London Ser. A* **1982**, *381*, 117.
(32) Lee, A. L.; Wand, A. J. *Nature* **2001**, *411*, 501.
(33) Zerbetto, M.; Polimeno, A.; Meirovitch, E. *J. Phys. Chem. B* **2009**, *113*, 13613.
(34) Moro, G. J.; Polimeno, A. *J. Chem. Phys.* **1997**, *107*, 7884.
(35) Brink, D. M.; Satchler, G. R. *Angular Momentum*; Clarendon Press: Oxford, UK, 1968.
(36) Xu, J.; Xue, Y.; Srynnikov, N. R. *J. Biomol. NMR* **2009**, *45*, 57.
(37) Chatfield, D. C.; Szabo, A.; Brooks, B. R. *J. Am. Chem. Soc.* **1998**, *120*, 5301.
(38) Spiegel, M. R.; Liu, J. *Mathematical Handbook of Formulas and Tables*, 2nd ed.; Schaum's Outline Series; McGraw-Hill: New York, 1999; p 266.
(39) Babu, Y. S.; Bugg, C. E.; Cook, W. J. *J. Mol. Biol.* **1988**, *204*, 191.
(40) Chatfield, D. C.; Augusten, A.; D'Cunha, C. *J. Biomol. NMR* **2004**, *29*, 377.
(41) Mandel, A. M.; Akke, M.; Palmer III, A. G. *J. Mol. Biol.* **1995**, *246*, 144.
(42) Batchelder, L. S.; Niu, C. H.; Torchia, D. A. *J. Am. Chem. Soc.* **1983**, *105*, 2228.
(43) Lee, A. L.; Kinnear, S. A.; Wand, A. J. *Nat. Struct. Biol.* **2000**, *7*, 72.
(44) Barnes, J. P.; Freed, J. H. *Biophys. J.* **1998**, *75*, 2532.
(45) Best, R. B.; Clarke, J.; Karplus, M. *J. Mol. Biol.* **2005**, *349*, 185.
(46) Vugmeyster, L.; Ostrovsky, D.; Ford, J. J.; Burton, S. D.; Lipton, A. S.; Hoatson, G. L.; Vold, R. L. *J. Am. Chem. Soc.* **2009**, *131*, 13651.
(47) Tamura, A.; Matsushita, M.; Naito, A.; Kojima, S.; Miura, K. I.; Akasaka, K. *Protein Sci.* **1996**, *5*, 127.
(48) Freed, J. H. *J. Chem. Phys.* **1977**, *66*, 4183.
(49) Johnson, E.; Palmer III, A. G.; Rance, M. *Proteins* **2007**, *66*, 796.
(50) Fuentes, E. J.; Gilmore, S. A.; Mauldin, R. V.; Lee, A. L. *J. Mol. Biol.* **2006**, *364*, 337.
(51) Clarkson, M. W.; Gilmore, S. A.; Edgell, M. H.; Lee, A. L. *Biochemistry* **2006**, *45*, 7693.
(52) Law, A. B.; Fuentes, E. J.; Lee, A. L. *J. Am. Chem. Soc.* **2009**, *131*, 6322.
(53) Petit, C. M.; Zhang, J.; Sapienza, P. J.; Fuentes, E. J.; Lee, A. L. *Proc. Natl. Acad. Sci. U.S.A.* **2009**, *106*, 18249.
(54) Zerbetto, M.; Polimeno, A.; Kotsyubynskyy, D.; Ghalebani, L.; Kowalewski, J.; Meirovitch, E.; Olsson, U.; Widmalm, G. *J. Chem. Phys.* **2009**, *131*, 234501.
(55) Barone, V.; Polimeno, A. *Phys. Chem. Chem. Phys.* **2006**, *8*, 4609.
(56) Barone, V.; Brustolon, M.; Cimino, P.; Polimeno, A.; Zerbetto, M.; Zoleo, A. *J. Am. Chem. Soc.* **2006**, *128*, 15865.
(57) Zerbetto, M.; Carlotto, S.; Polimeno, A.; Corvaja, C.; Franco, L.; Toniolo, C.; Formaggio, F.; Barone, V.; Cimino, P. *J. Phys. Chem. B* **2007**, *111*, 2668.
(58) Carlotto, S.; Cimino, P.; Zerbetto, M.; Franco, L.; Corvaja, C.; Crisma, M.; Formaggio, F.; Toniolo, C.; Polimeno, A.; Barone, V. *J. Am. Chem. Soc.* **2007**, *129*, 11248.
(59) Barone, V.; Polimeno, A. *Chem. Soc. Rev.* **2007**, *36*, 1724.
(60) Sezer, D.; Freed, J. H.; Roux, B. *J. Am. Chem. Soc.* **2009**, *131*, 2597.
(61) Sezer, D.; Freed, J. H.; Roux, B. *J. Chem. Phys.* **2008**, *128*, 165106.
(62) Sezer, D.; Freed, J. H.; Roux, B. *J. Phys. Chem. B* **2008**, *112*, 11014.
(63) Sezer, D.; Freed, J. H.; Roux, B. *J. Phys. Chem. B* **2008**, *112*, 5755.
(64) Prabhu, N. V.; Lee, A. L.; Wand, A. J.; Sharp, K. A. *Biochemistry* **2003**, *42*, 562.
(65) Henry, E.; Szabo, A. *J. Chem. Phys.* **1985**, *82*, 4753.
(66) Hu, H.; Hermans, J.; Lee, A. L. *J. Biomol. NMR* **2005**, *32*, 151.
(67) Showalter, S. A.; Johnson, E.; Rance, M.; Brüschweiler, R. *J. Phys. Chem. B* **2008**, *112*, 6203.

JP107130M